

# On the Distribution of SINR for MIMO Systems with Widely Linear MMSE Receivers

Wei Deng, *Student Member, IEEE*, Yili Xia, *Member, IEEE*, Zhe Li, *Member, IEEE*, and Wenjiang Pei

## Abstract

The widely linear least mean square error (WLMMSE) receiver has been an appealing option for multiple-input-multiple-output (MIMO) wireless systems, however, a statistical understanding on its pose-detection signal-to-interference-plus-noise ratio (SINR) in detail is still missing. To this end, we consider a WLMMSE MIMO transmission system over the uncorrelated Rayleigh fading channel and investigate the statistical properties of its SINR for an arbitrary antenna configuration with  $N_t$  transmit antennas and  $N_r$  receive ones. We first show that the SINR expression can be interpreted as the sum of  $N_t$  different and independent gamma random variables. Based on this finding, an analytic probability density function (PDF) of the SINR is exactly derived, in terms of the confluent hypergeometric function of the second kind, for WLMMSE MIMO systems with  $N_t = 2$  and 3, while for a more general case in practice, i.e.,  $N_t > 3$ , we resort to the moment generating function to obtain an approximate but closed form PDF, under some mild conditions. The so-derived PDFs further provide more physical insights into

This paper was presented in part at the IEEE International Symposium on Personal, Indoor and Mobile Radio Communications (PIMRC), London, U.K., Aug. 2020 [1].

W. Deng, Y. Xia and W. Pei are with the School of Information Science and Engineering, Southeast University, 2 Sipailou, Nanjing 210096, P. R. China. (e-mail: dengwei1@seu.edu.cn; yili\_xia@seu.edu.cn; wjpei@seu.edu.cn)

Z. Li is with the School of Electronic and Information Engineering, Soochow University, Suzhou 215006, China (e-mail: lizhe@suda.edu.cn)

WLMMSE MIMO receivers in terms of the outage probability, the symbol error rate, and the diversity gain, all presented in closed form. Monte Carlo simulations support the analysis.

### Index Terms

Multiple-input multiple-output (MIMO), widely-linear minimum mean square error (WLMMSE) receivers, signal-to-interference-and-noise ratio (SINR), outage probability, symbol error rate (SER), diversity gain.

## I. INTRODUCTION

In multiple-input-multiple-output (MIMO) communication systems, one of the main challenges for realizing spatial diversity and multiplexing is to find a computationally attractive alternative to the optimal receivers based on the principle of maximum likelihood [2], [3], as their complexity grow exponentially with the number of transceiver antennas [4]. One family of solutions to this issue are developed based on the linear minimum mean-square error (LMMSE) criterion [5], [6], which provide reliable data transmissions at polynomial computational complexity, and more importantly, serve as building blocks of more advanced communication schemes, such as the vertical Bell Laboratories layered space-time detector [7], and the recently developed sparsity-aware one in massive MIMO systems [8], [9].

Most LMMSE MIMO systems often assume that the complex-valued transmit signals have a vanishing complementary covariance matrix, whose statistical property is termed proper or second order circular [10], [11]. Interestingly, recent advances in the so-called augmented complex statistics have showed that, for improper transmit signals, additional performance gain can be achieved when both the received signal and its complex conjugate are jointly processed [12], [13]. This finding has spurred the extensive use of widely linear (WL) processing framework in numerous applications, where improper transmit signals appear due to their underlying generating physics [14]–[24]. Among these studies, many have assumed system models with real-valued

inputs [14]–[22]. This is because real-valued signals are not only essentially rectilinear ones with the maximal degree of impropriety [25], [26], but also they are popularly used in modulation schemes, such as amplitude-shift keying, binary phase-shift keying, and offset quadrature amplitude modulation, which are easily manipulated at low computational costs. For instance, the widely linear minimum mean-square error (WLMMSE) receiver proposed in [20] jointly exploits both the real-valued nature of the source symbols and the space-time structure of the Alamouti scheme to improve interference cancellation. In [21], a low-complexity WLMMSE precoding scheme was proposed for downlink large-scale MIMO systems. Moreover, in the context of multi-antenna radio frequency identification systems, enhanced anti-collision performance of the WLMMSE tag recovery method has been verified by real-world experiments [22].

To systematically understand the trade-off to determine the operating point within a MIMO receiver, its theoretical performance evaluation has long been a subject of interest, in which one of the most challenging tasks lies in characterizing statistical behaviors of the output signal-to-interference-plus-noise ratio (SINR). The SINR analysis of LMMSE receivers has been well established in the literature, including earlier works [27]–[29] which derived the asymptotic distribution of the SINR based on the well-known Gaussian assumption for the output noise, and more recent studies [30]–[32] which provided exact and explicit SINR distributions applicable to arbitrary antenna configurations. However, very few efforts [15], [18], have been devoted to theoretically investigate the SINR performance of the WLMMSE receiver. In [15], an adaptive WLMMSE detector has been developed in code division multiple access systems, and the analytic output SINR at steady state highlights the performance gain of the WL processing framework over its strictly linear counterpart. In [18], a WLMMSE demodulator was implemented in MIMO systems, and its concrete SINR expression was provided in a quadratic form, based on which an upper bound and an asymptotic evaluation on the average symbol error rate (SER) have been made possible. In short, the attempts in [15], [18] have addressed limited aspects on the performance of the WLMMSE receiver. To fill this void, we consider the WLMMSE MIMO

receiver with real-valued transmit signals, and investigate the statistical properties of its SINR in detail. The main contributions of this paper are summarized as follows:

- The SINR expression of a WLMMSE MIMO receiver with  $N_t$  transmit antennas and  $N_r$  receive antennas is rigorously derived in the uncorrelated Rayleigh fading environment. The eigenvalue analysis reveals that it can be interpreted as a sum of  $N_t$  different and independent gamma random variables (RVs). This result is different from that of the LMMSE MIMO receiver, which can be viewed as the sum of  $N_t - 1$  exponential RVs plus a chi-square RV [30]–[32]. The general PDF of the SINR is also provided, expressed in terms of the confluent Lauricella hypergeometric function.
- The so-derived PDF involves an  $(N_t - 1)$ -fold integral with the confluent Lauricella hypergeometric function in the integrand, making itself mathematically intractable to analyze. To this end, we follow the spirit of [30] to derive the exact and analytic PDFs of the SINR, which is applicable to WLMMSE MIMO systems with  $N_t = 2, 3$  and an arbitrary  $N_r$ .
- For the more general case, i.e.,  $N_t > 3$ , we alternatively resort to the moment generating function (MGF), and omit higher order terms of the Taylor-series expansion of the MGF, so as to yield an approximate PDF of the SINR. The resulting PDF is of a concise and closed form, and is valid for MIMO systems under rather mild conditions in practice.
- We make progress on the approximate PDF to elaborate its usefulness in typical MIMO system performance metrics, including outage probability, SER, and diversity gain. These closed form evaluations explain the simulated and experimental results in previous studies of WLMMSE estimators [18], [22], [33], and provide design guidelines for engineers in practice. Particularly, it is of great interest that the diversity gain improvement provided by the WLMMSE receiver over the LMMSE one is proved to linearly increase with the number of transmit antennas  $N_t$ .

This paper is organized as follows. In Section II, the WLMMSE estimator is briefly reviewed in

the context of point-to-point MIMO systems. In Section III, we evaluate the SINR performance of WLMSE MIMO systems, whereby the general, analytic and approximate PDFs are sequentially derived. In Section IV, the usefulness of our proposed SINR distribution analysis in MIMO system performance metrics is discussed. In Section V, the theoretical findings are verified through Monte Carlo simulations. Finally, Section VI concludes the paper.

*Notations:*

- Lowercase letters denote scalars,  $a$ , boldface letters column vectors,  $\mathbf{a}$ , and boldface uppercase letters matrices,  $\mathbf{A}$ . An  $N \times N$  identity matrix is denoted by  $\mathbf{I}_N$ . The superscripts  $(\cdot)^*$ ,  $(\cdot)^T$ ,  $(\cdot)^H$  and  $(\cdot)^{-1}$  denote respectively the complex conjugation, transpose, Hermitian transpose and matrix inversion operators. The operators  $\Re\{\cdot\}$  and  $\Im\{\cdot\}$  extract respectively the real and imaginary parts of a complex variable and  $j = \sqrt{-1}$ . The statistical expectation operator is denoted by  $E[\cdot]$ , while the operators  $\text{rank}\{\cdot\}$  and  $\text{Tr}\{\cdot\}$  return respectively the rank and the trace of a matrix. A diagonal matrix with scalar arguments is designated by  $\text{diag}\{\cdot\}$ , while the operators  $\min(\cdot)$  and  $\max(\cdot)$  return respectively the minimum and maximum of all entries. The operator  $\|\mathbf{a}\|$  and  $\|\mathbf{A}\|$  return respectively the Euclidean norm of the vector  $\mathbf{a}$  and the Frobenius norm of the matrix  $\mathbf{A}$ . For a matrix  $\mathbf{A} = [\mathbf{a}_1, \mathbf{a}_2, \dots, \mathbf{a}_n]$ , the matrix  $\mathbf{A}_{\langle j \rangle}$  denotes the one obtained by removing the  $j$ th column vector  $\mathbf{a}_j$  from  $\mathbf{A}$ , where  $j \in \{1, 2, \dots, n\}$ .
- $\mathcal{N}(\mathbf{a}, \mathbf{A})$  indicates a real-valued Gaussian distribution with mean  $\mathbf{a}$  and covariance  $\mathbf{A}$ , while  $\mathcal{CN}(\mathbf{b}, \mathbf{B})$  denotes a complex-valued circularly-symmetric Gaussian distribution with mean  $\mathbf{b}$  and covariance  $\mathbf{B}$ .  $\text{Gamma}(\alpha, \beta)$  represents a gamma distribution with a shape parameter  $\alpha$  and a scale parameter  $\beta$ .
- $\Gamma(a) = \int_0^\infty t^{a-1} e^{-t} dt$ ,  $\gamma(a, b) = \int_0^b t^{a-1} e^{-t} dt$  and  $\Gamma_b(a) = \pi^{b(b-1)/4} \prod_{i=1}^b \Gamma(a + (1-i)/2)$  represent respectively the gamma function, the incomplete gamma function and the multivariate gamma function. The rising factorial operation is denoted by  $(a)_b = \prod_{i=0}^{b-1} (a-i)$ . The Q-

function is represent by  $\mathcal{Q}(x) = \frac{1}{\sqrt{2\pi}} \int_x^{\infty} e^{-\frac{t^2}{2}} dt$ , where  $x \geq 0$ , and it computes the area under the tail of the normal distribution.

## II. SYSTEM MODEL

Let us consider a single point-to-point MIMO system with  $N_t$  transmitters and  $N_r$  receivers, where  $N_t \leq N_r$ . Then, the discrete-time baseband system model can be represented as

$$\mathbf{y} = \mathbf{H}\mathbf{x} + \mathbf{n}, \quad (1)$$

where  $\mathbf{y} \in \mathbb{C}^{N_r \times 1}$  is the received complex-valued vector,  $\mathbf{x} \triangleq [x_1, x_2, \dots, x_{N_t}]^T \in \mathbb{R}^{N_t \times 1}$  is the transmitted real-valued vector,  $\mathbf{H} \triangleq [\mathbf{h}_1, \mathbf{h}_2, \dots, \mathbf{h}_{N_t}] \in \mathbb{C}^{N_r \times N_t}$  is a channel gain matrix with each column vector  $\mathbf{h}_j$  representing the channels from the  $j$ th transmit antenna to all receive antennas, where  $1 \leq j \leq N_t$ , and  $\mathbf{n} \in \mathbb{C}^{N_r \times 1}$  is the complex noise vector subject to  $\mathcal{CN}(\mathbf{0}, \sigma^2 \mathbf{I}_{N_r})$ . We assume the entry in the  $i$ th row, where  $1 \leq i \leq N_r$ , and  $j$ th column of the channel gain matrix  $\mathbf{H}$ ,  $h_{i,j}$ , conform to i.i.d. standard complex-valued Normal distribution, i.e.,  $h_{i,j} \sim \mathcal{CN}(0, 1)$ , and the transmit power  $E_s$  is distributed equally over the transmit antennas, such that  $E[\mathbf{x}\mathbf{x}^T] = \frac{E_s}{N_t} \mathbf{I}_{N_t}$ .

In order to estimate the transmitted symbol  $x_j$  on the  $j$ th spatial stream from a complex-valued observation vector  $\mathbf{y}$ , the optimal WL processing framework is adopted, based on both  $\mathbf{y}$  and its conjugate counterpart  $\mathbf{y}^*$ , to give [12]

$$\hat{x}_j = \mathbf{w}_1^H \mathbf{y} + \mathbf{w}_2^H \mathbf{y}^*, \quad (2)$$

where  $\hat{x}_j$  is the received data on the  $j$ th spatial stream,  $\mathbf{w}_1$  and  $\mathbf{w}_2 \in \mathbb{C}^{N_r \times 1}$  are weight coefficient vectors. For compactness, (2) can be rewritten in an augmented form as

$$\hat{x}_j = \bar{\mathbf{w}}^H \bar{\mathbf{y}}, \quad (3)$$

where  $\bar{\mathbf{w}} \triangleq [\mathbf{w}_1^T, \mathbf{w}_2^T]^T \in \mathbb{C}^{2N_r \times 1}$  and  $\bar{\mathbf{y}} \triangleq [\mathbf{y}^T, \mathbf{y}^H]^T \in \mathbb{C}^{2N_r \times 1}$  are respectively the augmented weight coefficient vector and the augmented observation vector. The aim of the WLMSE

estimator is to find the optimal weight coefficient vector that minimizes the estimation error  $e_j$  in the mean square sense, that is,  $E[\|e_j\|^2]$ , where  $e_j \triangleq x_j - \hat{x}_j$ . According to [12], the optimal weight coefficient vector, denoted by  $\bar{\mathbf{w}}^o$ , is formulated as

$$\bar{\mathbf{w}}^o = \mathbf{R}_{\bar{\mathbf{y}}}^{-1} \mathbf{r}_{x_j \bar{\mathbf{y}}}, \quad (4)$$

where

$$\mathbf{R}_{\bar{\mathbf{y}}} \triangleq E[\bar{\mathbf{y}} \bar{\mathbf{y}}^H] = \frac{E_s}{N_t} \bar{\mathbf{H}} \bar{\mathbf{H}}^H + \sigma^2 \mathbf{I}_{2N_r}, \quad (5)$$

is the covariance matrix of the augmented observation vector  $\bar{\mathbf{y}}$ , and

$$\mathbf{r}_{x_j \bar{\mathbf{y}}} \triangleq E[x_j \bar{\mathbf{y}}] = \frac{E_s}{N_t} \bar{\mathbf{h}}_j, \quad (6)$$

is the cross correlation vector between the  $j$ th transmitted symbol  $x_j$  and the augmented observation vector  $\bar{\mathbf{y}}$ . The matrix  $\bar{\mathbf{H}} \in \mathbb{C}^{2N_r \times N_t}$  is defined as  $\bar{\mathbf{H}} \triangleq [\mathbf{H}^T, \mathbf{H}^H]^T$ , so that the Hermitian matrix  $\bar{\mathbf{H}} \bar{\mathbf{H}}^H$  in (5) can be decomposed as

$$\bar{\mathbf{H}} \bar{\mathbf{H}}^H = \begin{bmatrix} \mathbf{H} \mathbf{H}^H & \mathbf{H} \mathbf{H}^T \\ \mathbf{H}^* \mathbf{H}^H & \mathbf{H}^* \mathbf{H}^T \end{bmatrix}.$$

The column vector  $\bar{\mathbf{h}}_j \triangleq [\mathbf{h}_j^T, \mathbf{h}_j^H]^T \in \mathbb{C}^{2N_r \times 1}$  in (6) is the  $j$ th augmented channel column vector. A substitution of (4) into (3) yields the WMMSE solution, given by

$$\hat{x}_j = \frac{E_s}{N_t} \bar{\mathbf{h}}_j^H \left( \frac{E_s}{N_t} \bar{\mathbf{H}} \bar{\mathbf{H}}^H + \sigma^2 \mathbf{I}_{2N_r} \right)^{-1} \bar{\mathbf{y}} = \epsilon_j x_j + \xi_j, \quad (7)$$

where the coefficient of the signal component  $\epsilon_j$  and the interference-plus-noise component  $\xi_j$  are respectively defined as

$$\epsilon_j \triangleq \bar{\mathbf{h}}_j^H (\bar{\mathbf{H}} \bar{\mathbf{H}}^H + \rho^{-1} \mathbf{I}_{2N_r})^{-1} \bar{\mathbf{h}}_j, \quad (8)$$

$$\xi_j \triangleq \bar{\mathbf{h}}_j^H (\bar{\mathbf{H}} \bar{\mathbf{H}}^H + \rho^{-1} \mathbf{I}_{2N_r})^{-1} (\bar{\mathbf{y}} - x_j \bar{\mathbf{h}}_j). \quad (9)$$

The coefficient  $\rho$  in (8) and (9) is defined as  $\rho \triangleq E_s / (\sigma^2 N_t)$ , evaluating the average signal-to-noise ratio (SNR) per symbol per antenna.

### III. ANALYSIS ON THE SINR OF THE WLMMSE MIMO SYSTEM AND ITS DISTRIBUTION

In this section, we aim to study the post-detection SINR performance of the MIMO system with the WLMMSE detector in (7). By virtue of the random matrix theory [34], we first give the general distribution of the SINR, based on which, an exact analytic PDF of the SINR in case of a small number of transmit antennas, as well as an approximate closed-form one in the context of arbitrary antenna configurations, are subsequently provided.

#### A. SINR and Its General Distribution

Let us use  $\tau_j$  to denote the output SINR of the WLMMSE detector on the  $j$ th spatial stream. Then from (7),  $\tau_j$  is defined as

$$\tau_j \triangleq \frac{E[|\epsilon_j x_j|^2]}{E[|\xi_j|^2]}. \quad (10)$$

Based on (8) and (9), and after some mathematical manipulations, the SINR coefficient  $\tau_j$  in (10) becomes

$$\tau_j = \frac{\bar{\mathbf{h}}_j^H \mathbf{R}_{\bar{\mathbf{y}}}^{-1} \bar{\mathbf{h}}_j}{1 - \bar{\mathbf{h}}_j^H \mathbf{R}_{\bar{\mathbf{y}}}^{-1} \bar{\mathbf{h}}_j}. \quad (11)$$

To make the term on the right hand side (RHS) of (11) more mathematically tractable, for the WLMMSE estimate on the  $j$ th spatial stream,  $\hat{x}_j$ , we define its interference matrix  $\bar{\mathbf{C}}_j \triangleq \bar{\mathbf{H}}_{\langle i \rangle} \bar{\mathbf{H}}_{\langle i \rangle}^H \in \mathbb{C}^{2N_r \times 2N_r}$ , where  $\bar{\mathbf{H}}_{\langle i \rangle} \in \mathbb{C}^{2N_r \times (N_t - 1)}$ , and its interference-plus-noise matrix  $\bar{\mathbf{T}}_j \triangleq (\bar{\mathbf{C}}_j + \rho^{-1} \mathbf{I}_{2N_r}) \in \mathbb{C}^{2N_r \times 2N_r}$ . In this way, the matrix  $\mathbf{R}_{\bar{\mathbf{y}}}^{-1}$  in (11) can be written in terms of  $\bar{\mathbf{T}}_j$  as

$$\mathbf{R}_{\bar{\mathbf{y}}}^{-1} = (\bar{\mathbf{C}}_j + \bar{\mathbf{h}}_j \bar{\mathbf{h}}_j^H + \rho^{-1} \mathbf{I}_{2N_r})^{-1} = (\bar{\mathbf{T}}_j + \bar{\mathbf{h}}_j \bar{\mathbf{h}}_j^H)^{-1}. \quad (12)$$

Upon substituting (12) into (11), and exploiting the Woodbury's identity [35], the nominator

on the RHS of (11) can be derived as

$$\begin{aligned}
\bar{\mathbf{h}}_j^H \mathbf{R}_{\bar{\mathbf{y}}}^{-1} \bar{\mathbf{h}}_j &= \bar{\mathbf{h}}_j^H (\bar{\mathbf{T}}_j + \bar{\mathbf{h}}_j \bar{\mathbf{h}}_j^H)^{-1} \bar{\mathbf{h}}_j \\
&= \bar{\mathbf{h}}_j^H \left( \bar{\mathbf{T}}_j^{-1} - \frac{\bar{\mathbf{T}}_j^{-1} \bar{\mathbf{h}}_j \bar{\mathbf{h}}_j^H \bar{\mathbf{T}}_j^{-1}}{1 + \bar{\mathbf{h}}_j^H \bar{\mathbf{T}}_j^{-1} \bar{\mathbf{h}}_j} \right) \bar{\mathbf{h}}_j \\
&= \frac{\bar{\mathbf{h}}_j^H \bar{\mathbf{T}}_j^{-1} \bar{\mathbf{h}}_j}{1 + \bar{\mathbf{h}}_j^H \bar{\mathbf{T}}_j^{-1} \bar{\mathbf{h}}_j}.
\end{aligned} \tag{13}$$

Taking (13) into (11), we have

$$\tau_j = \bar{\mathbf{h}}_j^H \bar{\mathbf{T}}_j^{-1} \bar{\mathbf{h}}_j = \bar{\mathbf{h}}_j^H (\bar{\mathbf{C}}_j + \rho^{-1} \mathbf{I}_{2N_r})^{-1} \bar{\mathbf{h}}_j. \tag{14}$$

A direct inspection of (14) shows that statistical properties of the eigenvalues of the interference matrix  $\bar{\mathbf{C}}_j$  are prerequisites for the distribution analysis on the SINR coefficient  $\tau_j$ . To address this issue, we first exploit the duality between the complex-valued signal representation and its bivariate-real counterpart to rewrite the matrix  $\bar{\mathbf{H}}_{\langle j \rangle}$  as [10]

$$\bar{\mathbf{H}}_{\langle j \rangle} = \mathbf{J} \tilde{\mathbf{H}}_{\langle j \rangle}, \tag{15}$$

where

$$\mathbf{J} \triangleq \begin{bmatrix} \mathbf{I}_{N_r} & \mathcal{J} \mathbf{I}_{N_r} \\ \mathbf{I}_{N_r} & -\mathcal{J} \mathbf{I}_{N_r} \end{bmatrix}, \tag{16}$$

is the real-to-complex transformation matrix, and  $\tilde{\mathbf{H}}_{\langle j \rangle} \triangleq \left[ (\Re\{\mathbf{H}_{\langle j \rangle}\})^T, (\Im\{\mathbf{H}_{\langle j \rangle}\})^T \right]^T \in \mathbb{R}^{2N_r \times (N_t-1)}$  is a real composite matrix constructed by concatenating the real and imaginary parts of the matrix  $\mathbf{H}_{\langle j \rangle}$ .

Applying the Hermitian transpose operation on both sides of (15) and post-multiplying the result with (15), we have

$$\bar{\mathbf{C}}_j = \mathbf{J} \tilde{\mathbf{H}}_{\langle j \rangle} \tilde{\mathbf{H}}_{\langle j \rangle}^T \mathbf{J}^H = \mathbf{J} \tilde{\mathbf{C}}_j \mathbf{J}^H, \tag{17}$$

where the real composite interference matrix  $\tilde{\mathbf{C}}_j \triangleq \tilde{\mathbf{H}}_{\langle j \rangle} \tilde{\mathbf{H}}_{\langle j \rangle}^T \in \mathbb{R}^{2N_r \times 2N_r}$ . Since  $N_r \geq N_t$ , it is clear that  $\text{rank}\{\mathbf{H}\} = \text{rank}\{\bar{\mathbf{H}}\} = N_t$ , and consequently,  $\text{rank}\{\tilde{\mathbf{C}}_j\} = \text{rank}\{\tilde{\mathbf{H}}_{\langle j \rangle}\} = N_t - 1$ .

Now, applying the standard eigenvalue decomposition on  $\tilde{\mathbf{C}}_j$ , we have

$$\tilde{\mathbf{C}}_j = \mathbf{U} \Lambda \mathbf{U}^T, \quad (18)$$

where  $\mathbf{U} \in \mathbb{R}^{2N_r \times 2N_r}$  is an orthogonal matrix, and  $\Lambda \in \mathbb{R}^{2N_r \times 2N_r}$  is a diagonal matrix, given by

$$\Lambda = \text{diag}\left\{\lambda_1, \lambda_2, \dots, \lambda_{N_t-1}, \underbrace{0, \dots, 0}_{2N_r-N_t+1}\right\}, \quad (19)$$

which contains the ordered positive eigenvalues of the real composite interference matrix  $\tilde{\mathbf{C}}_j$ , i.e.,  $\lambda_1 > \lambda_2 > \dots > \lambda_{N_t-1} > 0$ .

After taking (18) into (17), the interference matrix  $\bar{\mathbf{C}}_j$  becomes

$$\bar{\mathbf{C}}_j = \mathbf{J} \mathbf{U} \Lambda \mathbf{U}^T \mathbf{J}^H = \mathbf{V} \Lambda \mathbf{V}^H, \quad (20)$$

where  $\mathbf{V} \triangleq \mathbf{J} \mathbf{U}$ , and hence from (14), we have

$$\begin{aligned} \tau_j &= \bar{\mathbf{h}}_j^H (\mathbf{V} \Lambda \mathbf{V}^H + \frac{1}{2\rho} \mathbf{V} \mathbf{V}^H)^{-1} \bar{\mathbf{h}}_j \\ &= (\mathbf{V}^H \bar{\mathbf{h}}_j)^H (\Lambda + \frac{1}{2\rho} \mathbf{I}_{2N_r})^{-1} (\mathbf{V}^H \bar{\mathbf{h}}_j) \\ &= \hat{\mathbf{h}}_j^H (\Lambda + \frac{1}{2\rho} \mathbf{I}_{2N_r})^{-1} \hat{\mathbf{h}}_j \\ &= \sum_{k=1}^{N_t-1} \frac{1}{\lambda_k + 1/(2\rho)} \hat{h}_{k,j}^2 + 2\rho \sum_{k=N_t}^{2N_r} \hat{h}_{k,j}^2, \end{aligned} \quad (21)$$

with the  $2N_r \times 1$  column vector  $\hat{\mathbf{h}}_j$  defined as

$$\hat{\mathbf{h}}_j \triangleq \mathbf{V}^H \bar{\mathbf{h}}_j = [\hat{h}_{1,j}, \hat{h}_{2,j}, \dots, \hat{h}_{2N_r,j}]^T. \quad (22)$$

Let  $\tilde{\mathbf{h}}_j \triangleq \mathbf{J}^H \bar{\mathbf{h}}_j$  denote the real-valued  $2N_r \times 1$  composite vector formed by concatenating the real and imaginary parts of the complex-valued channel vector  $\mathbf{h}_j$ , that is,

$$\tilde{\mathbf{h}}_j = \left[ \Re\{\mathbf{h}_j\}^T, \Im\{\mathbf{h}_j\}^T \right]^T = [\tilde{h}_{1,j}, \tilde{h}_{2,j}, \dots, \tilde{h}_{2N_r,j}]^T. \quad (23)$$

Then  $\hat{\mathbf{h}}_j$  and  $\tilde{\mathbf{h}}_j$  are related by

$$\hat{\mathbf{h}}_j = \mathbf{V}^H \bar{\mathbf{h}}_j = (\mathbf{J} \mathbf{U})^H \bar{\mathbf{h}}_j = \mathbf{U}^H \tilde{\mathbf{h}}_j. \quad (24)$$

Since the matrix  $\mathbf{U}$  is orthogonal,  $\hat{\mathbf{h}}_j$  preserves the exactly same statistical property as  $\tilde{\mathbf{h}}_j$ . Recall that the entries in the channel gain matrix  $\mathbf{H}$ ,  $h_{i,j} \sim \mathcal{CN}(0, 1)$ , so that the entries of the column vector  $\tilde{\mathbf{h}}_j$ ,  $\tilde{h}_{k,j} \sim \mathcal{N}(0, 1/2)$ , and consequently,  $\hat{h}_{k,j} \sim \mathcal{N}(0, 1/2)$ . Based on this finding, we further introduce the gamma RV, whose definition is provided in Appendix A, to interpret the SINR  $\tau_j$  in (21) as follows.

*Remark 1:* Given the eigenvalues  $\lambda_1, \lambda_2, \dots, \lambda_{N_t-1}$ , the first term on the RHS of (21) is a linear combination of  $N_t-1$  independent gamma RVs, each of which is subject to  $\text{Gamma}(1/2, \frac{2}{2\lambda_k+\rho^{-1}})$ , and the second term on the RHS of (21) is also a gamma RV subject to  $\text{Gamma}(\frac{2N_r-N_t+1}{2}, 2\rho)$ . In a word, the SINR  $\tau_j$  is a summation of  $N_t$  independent gamma RVs, in which the shape parameter  $\alpha_k$  and the scale parameter  $\beta_k$  of the  $k$ th gamma RV  $Z_k \sim \text{Gamma}(\alpha_k, \beta_k)$  are given by

$$\alpha_k = \begin{cases} 1/2 & 1 \leq k \leq N_t-1 \\ (2N_r-N_t+1)/2 & k=N_t \end{cases}, \quad \beta_k = \begin{cases} 2/(2\lambda_k+\rho^{-1}) & 1 \leq k \leq N_t-1 \\ 2\rho & k=N_t \end{cases}. \quad (25)$$

This result is different from the output SINR of the LMMSE detector in [30], [32], which has been proven to be the sum of  $N_t-1$  exponential RVs plus a chi-square RV, and hence a fundamentally different SINR distribution of the WLMSE detector is expected.

Based on the above discussion, we shall now investigate the general PDF of the output SINR  $\tau_j$ . Let  $f(\tau_j | \lambda_1, \lambda_2, \dots, \lambda_{N_t-1})$  be the joint conditional PDF of  $\tau_j$ , given the eigenvalues  $\lambda_1, \lambda_2, \dots, \lambda_{N_t-1}$ , then according to *Remark 1*,  $f(\tau_j | \lambda_1, \lambda_2, \dots, \lambda_{N_t-1})$  is the convolution of PDFs of the  $N_t$  gamma RVs,  $Z_1, Z_2, \dots, Z_{N_t}$ . Therefore, upon substituting (25) into (62) in Appendix A and convolving the results, the joint conditional PDF  $f(\tau_j | \lambda_1, \lambda_2, \dots, \lambda_{N_t-1})$  can be described as

$$f(\tau_j | \lambda_1, \lambda_2, \dots, \lambda_{N_t-1}) = \frac{\tau_j^{N_r-1} e^{-\frac{\tau_j}{\beta_1}}}{\prod_{k=1}^{N_t} \beta_k^{\alpha_k} \Gamma(N_r)} \times \Phi_2^{(N_t-1)} \left( \alpha_2, \alpha_3, \dots, \alpha_{N_t}; N_r; \left( \frac{1}{\beta_1} - \frac{1}{\beta_2} \right) \tau_j, \left( \frac{1}{\beta_1} - \frac{1}{\beta_3} \right) \tau_j, \dots, \left( \frac{1}{\beta_1} - \frac{1}{\beta_{N_t}} \right) \tau_j \right), \quad (26)$$

where the confluent Lauricella hypergeometric function  $\Phi_2^{(n)}(\cdot; \cdot; \cdot)$  is defined as [36, Eq. (36)]

$$\Phi_2^{(n)}(b_1, b_2, \dots, b_n; c; x_1, x_2, \dots, x_n) \triangleq \sum_{i_1, \dots, i_n=0}^{\infty} \frac{(b_1)_{i_1} (b_2)_{i_2} \dots (b_n)_{i_n} x_1^{i_1} x_2^{i_2} \dots x_n^{i_n}}{(c)_{i_1+i_2+\dots+i_n} i_1! i_2! \dots i_n!}. \quad (27)$$

On the other hand, according to [37, Theorem 1.3.22], the positive eigenvalues of the real composite interference matrix  $\tilde{\mathbf{C}}_j = \tilde{\mathbf{H}}_{\langle j \rangle} \tilde{\mathbf{H}}_{\langle j \rangle}^T$ , that is,  $\lambda_1, \lambda_2, \dots, \lambda_{N_t-1}$ , are exactly those of the real-valued Wishart matrix  $\tilde{\mathbf{H}}_{\langle j \rangle}^T \tilde{\mathbf{H}}_{\langle j \rangle} \sim \mathcal{W}_{N_t-1}(\frac{1}{2}\mathbf{I}_{N_t-1}, 2N_r)$ . Therefore, based on (63) in Appendix B, the joint PDF of the ordered positive eigenvalues  $\lambda_1, \lambda_2, \dots, \lambda_{N_t-1}$ , denoted by  $f_{\Lambda}(\lambda_1, \lambda_2, \dots, \lambda_{N_t-1})$ , can be expressed as

$$f_{\Lambda}(\lambda_1, \lambda_2, \dots, \lambda_{N_t-1}) = \frac{\pi^{(N_t-1)^2/2}}{\Gamma_{N_t-1}(N_r) \Gamma_{N_t-1}(\frac{N_t-1}{2})} \prod_{k=1}^{N_t-1} e^{-\lambda_k} (\lambda_k)^{N_r - \frac{N_t}{2}} \prod_{k < l}^{N_t-1} (\lambda_k - \lambda_l). \quad (28)$$

Finally, by considering (26) and (28), the general PDF of  $\tau_j$  can be derived by marginalization as

$$f(\tau_j) = \int_0^{\infty} \int_0^{\lambda_1} \dots \int_0^{\lambda_{N_t-2}} f(\tau_j | \lambda_1, \lambda_2, \dots, \lambda_{N_t-1}) f_{\Lambda}(\lambda_1, \lambda_2, \dots, \lambda_{N_t-1}) d\lambda_{N_t-1} \dots d\lambda_2 d\lambda_1. \quad (29)$$

### B. Analytic SINR Distribution for $N_r \times 2$ and $N_r \times 3$ WLMMSE MIMO Systems

Since the algebraic computation on the RHS of (29) involves an  $(N_t - 1)$ -fold integral, and the integrand  $f(\tau_j | \lambda_1, \lambda_2, \dots, \lambda_{N_t-1})$  in (26) contains the confluent Lauricella hypergeometric function  $\Phi_2^{(n)}(\cdot; \cdot; \cdot)$  which prohibits a simple integral representation [38], [39], the general PDF  $f(\tau_j)$  is mathematically intractable even with some advanced integration computing tools, such as Matlab and Mathematica. However, for a small  $N_t$ , e.g.,  $N_t = 2, 3$ , the confluent Lauricella hypergeometric function  $\Phi_2^{(n)}(\cdot; \cdot; \cdot)$  reduces to the confluent hypergeometric function of the first kind [40], based on which the exact and analytic PDF of  $\tau_j$  can be obtained. To that end, we first consider (29) in the simple case when  $N_t = 2$ , and the PDF of  $\tau_j$  for  $N_t = 3$  can be derived in a similar fashion.

Within a  $N_r \times 2$  MIMO system, the real-valued Wishart matrix  $\tilde{\mathbf{H}}_{\langle j \rangle}^T \tilde{\mathbf{H}}_{\langle j \rangle}$  collapses to a gamma RV with a shape parameter  $N_r$  and a scale parameter 1. In other words, there exists one single

positive eigenvalue  $\lambda$  in the real composite interference matrix  $\tilde{\mathbf{C}}_j$ , whose PDF  $f_{\Lambda}(\lambda)$  can be deduced from (62) in Appendix A as

$$f_{\Lambda}(\lambda) = \frac{1}{\Gamma(N_r)} \lambda^{N_r-1} e^{-\lambda}, \quad (30)$$

while the conditional PDF of  $\tau_j$ , given a single  $\lambda$ , can be deduced from (26) as

$$f_{N_r \times 2}(\tau_j | \lambda) = \frac{\tau_j^{N_r-1} e^{-\frac{\tau_j}{\beta_1}}}{\beta_1^{\alpha_1} \beta_2^{\alpha_2} \Gamma(N_r)} \Phi_2^{(1)} \left( \alpha_2; N_r; \left( \frac{1}{\beta_1} - \frac{1}{\beta_2} \right) \tau_j \right) = \frac{\tau_j^{N_r-1} e^{-\frac{\tau_j}{\beta_1}}}{\beta_1^{\alpha_1} \beta_2^{\alpha_2} \Gamma(N_r)} M \left( \alpha_2; N_r; \left( \frac{1}{\beta_1} - \frac{1}{\beta_2} \right) \tau_j \right), \quad (31)$$

where  $M(\cdot, \cdot, \cdot)$  is the confluent hypergeometric function of the first kind [40]. Upon using (25) to interpret the shape parameters  $\alpha_1, \alpha_2$  and the scale parameters  $\beta_1, \beta_2$ , from (31), we have

$$f_{N_r \times 2}(\tau_j | \lambda) = \frac{\tau_j^{N_r-1} e^{-\frac{2\lambda+\rho^{-1}}{2}\tau_j} \sqrt{2\lambda+\rho^{-1}}}{\Gamma(N_r) 2^{N_r} \rho^{N_r-\frac{1}{2}}} M \left( N_r - \frac{1}{2}, N_r, \lambda \tau_j \right). \quad (32)$$

Now, based on (30) and (32), the PDF of  $\tau_j$  for the  $N_r \times 2$  WLMMSE MIMO system can be computed by marginalization as

$$\begin{aligned} f_{N_r \times 2}(\tau_j) &= \int_0^{\infty} f_{N_r \times 2}(\tau_j | \lambda) f_{\Lambda}(\lambda) d\lambda \\ &= \frac{\tau_j^{N_r-1} e^{-\frac{\tau_j}{2\rho}}}{2^{N_r} (\Gamma(N_r))^2 \rho^{N_r-\frac{1}{2}}} \int_0^{\infty} \sqrt{2\lambda+\rho^{-1}} \lambda^{N_r-1} e^{-(1+\tau_j)\lambda} M \left( N_r - \frac{1}{2}, N_r, \lambda \tau_j \right) d\lambda. \end{aligned} \quad (33)$$

According to [40, Eq. 13.2.2], the confluent hypergeometric function of the first kind, that is,  $M(N_r - \frac{1}{2}, N_r, \lambda \tau_j)$ , allows the following infinite-series expansion

$$M \left( N_r - \frac{1}{2}, N_r, \lambda \tau_j \right) = \sum_{m=0}^{\infty} \frac{(N_r - \frac{1}{2})_m (\lambda \tau_j)^m}{(N_r)_m m!}. \quad (34)$$

A substitution of (34) into (33) yields

$$f_{N_r \times 2}(\tau_j) = \frac{\tau_j^{N_r-1} e^{-\frac{\tau_j}{2\rho}}}{2^{N_r} (\Gamma(N_r))^2 \rho^{N_r-\frac{1}{2}}} \sum_{m=0}^{\infty} \frac{(N_r - \frac{1}{2})_m \tau_j^m}{(N_r)_m m!} \underbrace{\int_0^{\infty} \sqrt{2\lambda+\rho^{-1}} \lambda^{N_r+m-1} e^{-(1+\tau_j)\lambda} d\lambda}_{g(m)}. \quad (35)$$

Observe that the integral term in (35),  $g(m)$ , is in fact the Mellin transform of the term,  $\sqrt{2\lambda+\rho^{-1}} \lambda^{N_r} e^{-(1+\tau_j)\lambda}$ , so that according to [41] and after some algebraic manipulations, the

function  $g(m)$  can be expressed as

$$g(m) = \frac{\Gamma(N_r + m)}{2^{N_r+m} \rho^{N_r+m+\frac{1}{2}}} U\left(N_r + m, N_r + m + \frac{3}{2}, \frac{\tau_j + 1}{2\rho}\right), \quad (36)$$

where  $U(\cdot, \cdot, \cdot)$  is the confluent hypergeometric function of the second kind [40].

Upon taking (36) into (35), we finally arrive at the analytical PDF of  $\tau_j$  for the  $N_r \times 2$  WLMSE MIMO system in the form of infinite series, given by

$$f_{N_r \times 2}(\tau_j) = \frac{\tau_j^{N_r-1} e^{-\frac{\tau_j}{2\rho}}}{(2\rho)^{2N_r} (\Gamma(N_r))^2} \sum_{m=0}^{\infty} \frac{(N_r - \frac{1}{2})_m \tau_j^m \Gamma(N_r + m)}{(N_r)_m 2^m \rho^m m!} U\left(N_r + m, N_r + m + \frac{3}{2}, \frac{\tau_j + 1}{2\rho}\right). \quad (37)$$

whose convergence is proved in Appendix C.

Similar to the analysis from (30) to (37), we can obtain the analytic PDF of  $\tau_j$  for  $N_t = 3$ , given by

$$f_{N_r \times 3}(\tau_j) = \frac{e^{-\frac{\tau_j}{2\rho}}}{\sqrt{2\rho}} \sum_{m_1=0}^{\infty} \sum_{m_2=0}^{\infty} \sum_{m_3=0}^{\infty} \sum_{m_4=0}^{\infty} \frac{(-1)^{m_3+m_4} (\frac{1}{2})_{m_1} (-\frac{1}{2})_{m_4} (N_r - 1)_{m_2} (N_r + m_3 - \frac{1}{2})_{m_4} \tau_j^{m_1+m_2}}{\sqrt{2} (N_r)_{m_1+m_2} (N_r + m_1 + m_3 + \frac{3}{2})_{m_4} \sum_{l=1}^4 (m_l)!} \\ \times \frac{\Gamma(m_1+2) \Gamma(N_r + m_3 - \frac{1}{2}) \Gamma\left(2N_r + \sum_{l=1}^4 m_l\right)}{\Gamma(N_r + m_1 + m_3 + \frac{3}{2}) (2\rho)^{2N_r + \sum_{i=1}^3 m_i}} U\left(2N_r + \sum_{l=1}^4 m_l, 2N_r + \sum_{l=1}^4 m_l + \frac{3}{2}, \frac{\tau_j + 1}{2\rho}\right). \quad (38)$$

### C. Approximate SINR Distribution for Arbitrary $N_r \times N_t$ WLMSE MIMO Systems

In general, the integral of a combination of confluent hypergeometric functions is mathematically intractable, limiting the applicability of  $f_{N_r \times 2}(\tau_j)$  and  $f_{N_r \times 3}(\tau_j)$  in practical MIMO performance metrics, such as outage probability and SER. Besides, the approach used to obtain  $f_{N_r \times 2}(\tau_j)$  and  $f_{N_r \times 3}(\tau_j)$ , unfortunately, does not fit the more general occasion, i.e.,  $N_t > 3$ . In this regard, we next exploit the moment generating function (MGF) of a gamma RV to derive an approximate PDF of the SINR  $\tau_j$  for WLMSE MIMO systems of arbitrary size.

As stated in *Remark 1*, the SINR  $\tau_j$  is composed by summing up  $N_t$  gamma RVs  $Z_1, Z_2, \dots, Z_{N_t}$ , therefore, by definition [42], its conditional MGF, given the eigenvalues  $\lambda_1, \lambda_2, \dots, \lambda_{N_t-1}$ , can be expressed as

$$G(s | \lambda_1, \lambda_2, \dots, \lambda_{N_t-1}) \triangleq \prod_{k=1}^{N_t} (1 - \beta_k s)^{-\alpha_k}, \quad (39)$$

which, after interpreting the shape parameter  $\alpha_k$  and the scale parameter  $\beta_k$  via (25), becomes

$$G(s|\lambda_1, \lambda_2, \dots, \lambda_{N_t-1}) = (1 - 2\rho s)^{-\frac{2N_r - N_t + 1}{2}} \prod_{k=1}^{N_t-1} \left(1 - \frac{2s}{2\lambda_k + \rho^{-1}}\right)^{-\frac{1}{2}}. \quad (40)$$

To make the RHS of (40) more mathematically tractable, we define  $\eta_k \triangleq (\lambda_k + \frac{1}{2}\rho^{-1})^{-1}$ , and apply the first-order Taylor series expansion to the  $k$ th factorial within the sequence product  $\prod_{k=1}^{N_t-1} \left(1 - \frac{2s}{2\lambda_k + \rho^{-1}}\right)^{-\frac{1}{2}}$ , to give

$$\left(1 - \frac{2s}{2\lambda_k + \rho^{-1}}\right)^{-\frac{1}{2}} = (1 - s\eta_k)^{-\frac{1}{2}} = 1 + \frac{s}{2}\eta_k + O(\eta_k), \quad (41)$$

where  $O(\eta_k)$  denotes the second and higher-power terms of  $\eta_k$ . According to the analysis in [43], when  $N_t \leq N_r$ , the expectation of the smallest eigenvalue of the real-valued Wishart matrix  $\mathcal{W}_{N_t-1}(\frac{1}{2}\mathbf{I}_{N_t-1}, 2N_r)$  is proven to be greater than unity, i.e.,  $\forall k \in 1, 2, \dots, N_t - 1$ ,  $\lambda_k > 1$ . Moreover, by definition, the SNR coefficient  $\rho > 0$ . Overall, we have  $0 < \eta_k < 1$ , which always guarantees a convergent Taylor series expansion in (41).

Now, upon taking (41) into (40) and ignoring the second and higher-power terms of  $\eta_k$ , the conditional MGF  $G(s|\lambda_1, \lambda_2, \dots, \lambda_{N_t-1})$  can be approximated as

$$G(s|\lambda_1, \lambda_2, \dots, \lambda_{N_t-1}) \approx (1 - 2\rho s)^{-\frac{2N_r - N_t + 1}{2}} \left(1 + \frac{s}{2} \sum_{k=1}^{N_t-1} \eta_k\right). \quad (42)$$

Based on (42) and (28), the approximate MGF of  $\tau_j$  can be derived by marginalization as

$$\begin{aligned} G(s) &= \int_0^\infty \int_0^{\lambda_1} \cdots \int_0^{\lambda_{N_t-2}} G(s|\lambda_1, \lambda_2, \dots, \lambda_{N_t-1}) f_{\mathbf{\Lambda}}(\lambda_1, \lambda_2, \dots, \lambda_{N_t-1}) d\lambda_{N_t-1} \cdots d\lambda_2 d\lambda_1 \\ &\approx (1 - 2\rho s)^{-\frac{2N_r - N_t + 1}{2}} \int_0^\infty \int_0^{\lambda_1} \cdots \int_0^{\lambda_{N_t-2}} \left(1 + \frac{s}{2} \sum_{k=1}^{N_t-1} \eta_k\right) f_{\mathbf{\Lambda}}(\lambda_1, \lambda_2, \dots, \lambda_{N_t-1}) d\lambda_{N_t-1} \cdots d\lambda_2 d\lambda_1 \\ &= (1 - 2\rho s)^{-\frac{2N_r - N_t + 1}{2}} (1 + G_0 s), \end{aligned} \quad (43)$$

where

$$G_0 = \frac{1}{2} \int_0^\infty \int_0^{\lambda_1} \cdots \int_0^{\lambda_{N_t-2}} \sum_{k=1}^{N_t-1} \eta_k f_{\mathbf{\Lambda}}(\lambda_1, \lambda_2, \dots, \lambda_{N_t-1}) d\lambda_{N_t-1} \cdots d\lambda_2 d\lambda_1. \quad (45)$$

Moreover, the variable  $\eta_k$  in (45) can be further approximated as  $\eta_k = (\lambda_k + \frac{1}{2}\rho^{-1})^{-1} \approx \lambda_k^{-1}$  when the eigenvalue  $\lambda_k \gg \frac{1}{2}\rho^{-1}$ . This is a mild condition in practice, which is achievable either when the SNR  $\rho$  is sufficiently high or when the number of receive antennas  $N_r$  is sufficiently greater than<sup>1</sup>  $\frac{N_t-1}{2}$ . With the approximated  $\eta_k$  in hand, the quantity  $G_0$  in (45) simplifies into

$$\begin{aligned} G_0 &\approx \int_0^\infty \int_0^{\lambda_1} \cdots \int_0^{\lambda_{N_t-2}} \left( \sum_{k=1}^{N_t-1} \frac{1}{\lambda_k} \right) f_{\mathbf{\Lambda}}(\lambda_1, \lambda_2, \dots, \lambda_{N_t-1}) d\lambda_{N_t-1} \cdots d\lambda_2 d\lambda_1 \\ &= \frac{1}{2} E[\text{Tr}\{\tilde{\mathbf{C}}_j^{-\mathcal{T}}\}] = \frac{1}{2} \text{Tr}\{E[\tilde{\mathbf{C}}_j^{-\mathcal{T}}]\} \end{aligned} \quad (46)$$

$$= \frac{1}{2} \text{Tr} \left\{ \frac{2}{2N_r - N_t} \mathbf{I}_{N_t-1} \right\} = \frac{N_t - 1}{2N_r - N_t}, \quad (47)$$

in which the step from (46) to (47) is achieved by exploiting [44, Theorem 3.1 (i)].

Upon substituting (47) into (44), the approximate MGF of  $\tau_j$  becomes

$$G(s) \approx (1 - 2\rho s)^{-\frac{2N_r - N_t + 1}{2}} \left( 1 + \frac{N_t - 1}{2N_r - N_t} s \right), \quad (48)$$

based on which, applying the inverse Laplace transform and after some mathematical manipulations, the approximate PDF of  $\tau_j$ , denoted by  $f_a(\tau_j)$ , can be obtained in closed form as

$$f_a(\tau_j) \approx \left\{ 1 - \frac{N_t - 1}{2N_r - N_t} \left( \frac{2N_r - N_t - 1}{2\tau_j} - \frac{1}{2\rho} \right) \right\} \frac{(\tau_j)^{\frac{2N_r - N_t - 1}{2}} e^{-\frac{\tau_j}{2\rho}}}{(2\rho)^{\frac{2N_r - N_t + 1}{2}} \Gamma(\frac{2N_r - N_t + 1}{2})}. \quad (49)$$

*Remark 2:* By comparing (49) with (62) in Appendix A, we observe that the approximate PDF,  $f_a(\tau_j)$ , is the product of the term,  $1 - \frac{N_t - 1}{2N_r - N_t} \left( \frac{2N_r - N_t - 1}{2\tau_j} - \frac{1}{2\rho} \right)$ , and the PDF of a gamma RV with a shape parameter,  $\frac{2N_r - N_t - 1}{2}$ , and a scale parameter,  $2\rho$ . Since a gamma RV gradually turns to be Gaussian when its shape parameter approaches to infinity [45], it is expected that  $f_a(\tau_j)$  becomes a more Gaussian-like PDF as the difference between the number of receive antennas and that of transmit ones,  $2N_r - N_t$ , increases.

<sup>1</sup>For a real-valued Wishart matrix  $\tilde{\mathbf{C}}_j^{\mathcal{T}} \sim \mathcal{W}_{N_t-1}(\frac{1}{2}\mathbf{I}_{N_t-1}, 2N_r)$ , the expectation of its minimum eigenvalue is proven to monotonically increase with  $2N_r - N_t + 1$  [43].

#### IV. IMPORTANT APPLICATIONS AND DISCUSSIONS

In this section, we are focused on the usefulness of MGF and approximate PDF of the SINR derived in Section III-C in some practical MIMO system performance metrics, including outage probability, SER, and diversity gain, which theoretically explains the simulated and experimental results in previous studies on WLMMSE estimators [18], [22], [33].

##### A. Outage Probability Analysis

The outage probability on the  $j$ th spatial stream is defined as the probability that the SINR  $\tau_j$  drops below a certain threshold  $\tau_o$  [46], denoted as  $\Pr(\tau_j \leq \tau_o)$ . By computing the indefinite integral of the approximate PDF  $f_a(\tau_j)$  in (49), we have

$$\begin{aligned} \Pr(\tau_j \leq \tau_o) &= \int_0^{\tau_o} f(\tau_j) d\tau_j \\ &\approx \int_0^{\tau_o} \frac{(\tau_j)^{\frac{2N_r-N_t-1}{2}} e^{-\frac{\tau_j}{2\rho}}}{(2\rho)^{\frac{2N_r-N_t+1}{2}} \Gamma\left(\frac{2N_r-N_t+1}{2}\right)} \left\{ 1 - \frac{N_t-1}{2N_r-N_t} \left( \frac{2N_r-N_t-1}{2\tau_j} - \frac{1}{2\rho} \right) \right\} d\tau_j \\ &= \frac{\gamma\left(\frac{2N_r-N_t+1}{2}, \frac{\tau_o}{2\rho}\right)}{\Gamma\left(\frac{2N_r-N_t+1}{2}\right)} - \frac{(N_t-1)(\tau_o)^{\frac{2N_r-N_t-1}{2}} e^{-\frac{\tau_o}{2\rho}}}{(2N_r-N_t)(2\rho)^{\frac{2N_r-N_t+1}{2}} \Gamma\left(\frac{2N_r-N_t+1}{2}\right)}. \end{aligned} \quad (50)$$

Especially, when the value of  $2N_r - N_t$  becomes large, the second term on the RHS of (50) approaches zero, and consequently, the outage probability,  $\Pr(\tau_j \leq \tau_o)$ , becomes a normalized incomplete gamma function, i.e.,  $\frac{\gamma\left(\frac{2N_r-N_t+1}{2}, \frac{\tau_o}{2\rho}\right)}{\Gamma\left(\frac{2N_r-N_t+1}{2}\right)}$ .

##### B. SER Analysis

The SER represents the probability of transmitting a correct symbol but erroneously receiving its distorted version, and it can be formulated as a function of the SNR  $\rho$ , denoted by  $P_e(\rho)$ . Based on the law of total probability, the SER  $P_e(\rho)$  can be calculated by marginalization as

$$P_e(\rho) = \int_0^{\infty} P_e(\rho|\tau_j) f(\tau_j) d\tau_j, \quad (51)$$

where  $P_e(\rho|\tau_j)$  is the conditional SER given the SINR  $\tau_j$ . Based on the WLMMSE estimator in (7), the conditional SER  $P_e(\rho|\tau_j)$  can be obtained as [47, Eq. 5-2-5]

$$P_e(\rho|\tau_j) = \mathcal{Q} \left( \sqrt{\frac{E[|\epsilon_j x_j|^2]}{E[|\xi_j|^2]}} \right) = \mathcal{Q}(\sqrt{\tau_j}). \quad (52)$$

By considering a numerical approximation of the Q-function, that is [48]

$$\mathcal{Q}(x) \approx \frac{1}{12}e^{-\frac{x^2}{2}} + \frac{1}{4}e^{-\frac{2x^2}{3}}, \quad (53)$$

the conditional SER  $P(\rho|\tau_j)$  in (52) becomes

$$P_e(\rho|\tau_j) \approx \frac{1}{12}e^{-\frac{1}{2}\tau_j} + \frac{1}{4}e^{-\frac{2}{3}\tau_j}. \quad (54)$$

Upon substituting (54) into (51), and using (29) and (48), the approximate SER  $P_e(\rho)$  can be derived in closed form as

$$\begin{aligned} P_e(\rho) &= \int_0^\infty P_e(\rho|\tau_j) \int_0^{\lambda_1} \int_0^{\lambda_2} \cdots \int_0^{\lambda_{N_t-2}} f(\tau_j|\lambda_1, \lambda_2, \dots, \lambda_{N_t-1}) f_{\Lambda}(\lambda_1, \lambda_2, \dots, \lambda_{N_t-1}) d\lambda_{N_t-1} \cdots d\lambda_2 d\lambda_1 \\ &\approx \int_0^{\lambda_1} \int_0^{\lambda_2} \cdots \int_0^{\lambda_{N_t-2}} \left( \int_0^\infty \left( \frac{1}{12}e^{-\frac{1}{2}\tau_j} + \frac{1}{4}e^{-\frac{2}{3}\tau_j} \right) f(\tau_j|\lambda_1, \lambda_2, \dots, \lambda_{N_t-1}) d\tau_j \right) \\ &\quad \times f_{\Lambda}(\lambda_1, \lambda_2, \dots, \lambda_{N_t-1}) d\lambda_{N_t-1} \cdots d\lambda_2 d\lambda_1 \\ &= \int_0^{\lambda_1} \int_0^{\lambda_2} \cdots \int_0^{\lambda_{N_t-2}} \left[ \frac{1}{12}G\left(-\frac{1}{2}|\lambda_1, \lambda_2, \dots, \lambda_{N_t-1}\right) + \frac{1}{4}G\left(-\frac{2}{3}|\lambda_1, \lambda_2, \dots, \lambda_{N_t-1}\right) \right] \\ &\quad \times f_{\Lambda}(\lambda_1, \lambda_2, \dots, \lambda_{N_t-1}) d\lambda_{N_t-1} \cdots d\lambda_2 d\lambda_1 \\ &= \frac{4N_r - 3N_t + 1}{12(4N_r - 2N_t)} (1 + \rho)^{-\frac{2N_r - N_t + 1}{2}} + \frac{6N_r - 5N_t + 2}{4(6N_r - 3N_t)} \left(1 + \frac{4}{3}\rho\right)^{-\frac{2N_r - N_t + 1}{2}}. \end{aligned} \quad (55)$$

From (55), we observe that the approximate SER  $P_e(\rho)$  consists of two exponential functions, both of which decay at a rate of  $\frac{2N_r - N_t + 1}{2}$ .

### C. Diversity Gain Analysis

The diversity gain  $d$  of a MIMO system is defined as [49]

$$d = - \lim_{\rho \rightarrow \infty} \frac{P_e(\rho)}{\log \rho}. \quad (56)$$

According to [46, Eq. 5.3], the SER  $P_e(\rho)$  can be expressed in terms of the MGF of  $\tau_j$ ,  $G(s)$ , as

$$P_e(\rho) = \frac{1}{\pi} \int_0^{\pi/2} G\left(-\frac{1}{2\sin^2\theta}\right) d\theta. \quad (57)$$

Upon substituting (57) into (56) and exploiting (43), the diversity gain  $d$  becomes

$$\begin{aligned} d &= - \lim_{\rho \rightarrow \infty} \frac{\frac{1}{\pi} \int_0^{\pi/2} G\left(-\frac{1}{2\sin^2\theta}\right) d\theta}{\log \rho} \\ &= - \lim_{\rho \rightarrow \infty} \frac{\frac{1}{\pi} \int_0^{\pi/2} \left[ \int_0^{\lambda_1} \int_0^{\lambda_2} \cdots \int_0^{\lambda_{N_t-2}} G\left(-\frac{1}{2\sin^2\theta} | \lambda_1, \lambda_2, \dots, \lambda_{N_t-1}\right) f_{\Lambda}(\lambda_1, \lambda_2, \dots, \lambda_{N_t-1}) d\lambda_{N_t-1} \cdots d\lambda_2 d\lambda_1 \right] d\theta}{\log \rho} \\ &= - \int_0^{\infty} \int_0^{\lambda_1} \int_0^{\lambda_{N_t-2}} \left[ \underbrace{\lim_{\rho \rightarrow \infty} \frac{\frac{1}{\pi} \int_0^{\pi/2} G\left(-\frac{1}{2\sin^2\theta} | \lambda_1, \lambda_2, \dots, \lambda_{N_t-1}\right) d\theta}{\log \rho}}_{L(\rho)} \right] \\ &\quad \times f_{\Lambda}(\lambda_1, \lambda_2, \dots, \lambda_{N_t-1}) d\lambda_{N_t-1} \cdots d\lambda_2 d\lambda_1, \end{aligned} \quad (58)$$

where, by further considering (40), the term  $\lim_{\rho \rightarrow \infty} L(\rho)$  in (58) becomes

$$\begin{aligned} \lim_{\rho \rightarrow \infty} L(\rho) &= \lim_{\rho \rightarrow \infty} \frac{\log \left\{ \frac{1}{\pi} \rho^{-\frac{2N_r-N_t+1}{2}} \int_0^{\pi/2} \left( \frac{1}{\rho} + \frac{1}{\sin^2\theta} \right)^{-\frac{2N_r-N_t+1}{2}} \prod_{k=1}^{N_t-1} \left[ 1 + \frac{1}{(2\lambda_k + \rho^{-1})\sin^2\theta} \right]^{-1/2} d\theta \right\}}{\log \rho} \\ &= \lim_{\rho \rightarrow \infty} \frac{\log \left\{ \rho^{-\frac{2N_r-N_t+1}{2}} \right\} + \log \left\{ \frac{1}{\pi} \int_0^{\pi/2} \left( \frac{1}{\rho} + \frac{1}{\sin^2\theta} \right)^{-\frac{2N_r-N_t+1}{2}} \prod_{k=1}^{N_t-1} \left[ 1 + \frac{1}{(2\lambda_k + \rho^{-1})\sin^2\theta} \right]^{-1/2} d\theta \right\}}{\log \rho} \\ &= -N_r + \frac{N_t - 1}{2} + \lim_{\rho \rightarrow \infty} \frac{\log \left\{ \frac{1}{\pi} \int_0^{\pi/2} \left( \frac{1}{\sin^2\theta} \right)^{-\frac{2N_r-N_t+1}{2}} \prod_{k=1}^{N_t-1} \left[ 1 + \frac{1}{2\lambda_k \sin^2\theta} \right]^{-1/2} d\theta \right\}}{\log \rho} \\ &= -N_r + \frac{N_t - 1}{2}. \end{aligned} \quad (59)$$

A substitution of (59) into (58) yields

$$d = N_r - \frac{N_t - 1}{2}. \quad (60)$$

*Remark 3:* Unlike the outage probability  $\Pr(\tau_j \leq \tau_0)$  in (50) and the SER  $P_e(\rho)$  in (55), the diversity gain  $d$  in (60) is an exact value for WLMMSE MIMO systems with real-valued transmit signals since its derivation does not involve any approximation. This diversity gain  $d$  is also the decaying rate of the exponential functions involved in the SER  $P_e(\rho)$  in (55). Recall that the diversity gain for the conventional LMMSE MIMO systems is given by  $d_{\text{LMMSE}} = N_r - N_t + 1$  [30], [32], hence the diversity gain improvement introduced by a WLMMSE receiver, denoted by  $\Delta d$ , can be quantified as

$$\Delta d \triangleq d - d_{\text{LMMSE}} = N_r - \frac{N_t - 1}{2} - (N_r - N_t + 1) = \frac{N_t - 1}{2}, \quad (61)$$

and this improvement linearly increases with the number of transmit antennas  $N_t$ .

## V. SIMULATIONS

Numerical simulations were provided to validate our theoretical performance analysis on WLMMSE MIMO systems. Throughout the simulations, the transmitted real-valued symbols in  $\mathbf{x}$  were BPSK modulated, and the transmit power was set to  $E_s = 1$ . Each entry of the channel gain matrix  $\mathbf{H}$  was modeled by i.i.d. standard complex Normal distribution, i.e.,  $h_{i,j} \sim \mathcal{CN}(0, 1)$ .

In the first set of simulations, the validity of the analytic PDF of the SINR was examined for  $N_r \times 2$  MIMO systems. The SNR  $\rho$  was set to 0 dB, and three different antenna configurations,  $2 \times 2$ ,  $3 \times 2$  and  $4 \times 2$ , were considered for illustration purpose. The analytic  $f_{N_r \times 2}(\tau_j)$  was evaluated based on (37), in which the number of convergent series used to plot the analytic PDF,  $f_{2 \times 2}(\tau_j)$ ,  $f_{3 \times 2}(\tau_j)$  and  $f_{4 \times 2}(\tau_j)$ , was 30, 60 and 120, respectively, while the simulated PDF was illustrated by a histogram calculated from  $8 \times 10^5$  independent realizations for each antenna configuration. Observe in Fig. 1 that the analytic PDF spreads out away from the ordinate and becomes broader and shallower as the number of receive antennas,  $N_r$ , increases from 2 to 4. This

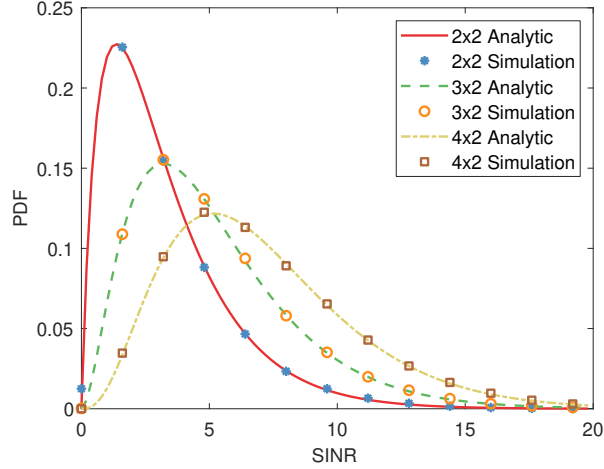


Fig. 1. Analytic and simulated PDFs  $f_{N_r \times 2}(\tau_j)$  as functions of the SINR.

is expected, because, given a fixed number of transmit antennas  $N_t$ , the SINR  $\tau_j$  mainly depends on the second term on the RHS of (21), whose expectation,  $E \left[ 2\rho \sum_{k=N_t}^{2N_r} \hat{h}_{k,j}^2 \right] = \rho(2N_r - N_t + 1)$ , monotonically increases against  $N_r$ . Moreover, the analytic and simulated PDFs are well matched for different SINR situations and antenna configurations.

In the next stage, we compared the approximate PDF  $f_a(\tau_j)$  in (49), with its numerical counterpart, which was illustrated by a histogram computed from  $8 \times 10^5$  independent realizations. In this experiment, we first considered a  $2 \times 2$  MIMO system, and set the SNR  $\rho = 0$  dB, 3 dB, 6 dB, 9 dB, respectively. As is shown in Fig. 2(a), when  $\rho = 0$  dB, the mismatch between the approximate and simulated PDFs appears around the peak of the PDF curve. However, when  $\rho \geq 3$  dB, the approximate PDFs are in good agreement with their respective numerical results in the entire SINR range. Next, we fixed the SNR  $\rho = 3$  dB, and examined the approximate PDF for small-scale and large-scale antenna configurations in Fig. 2(b) and Fig. 2(c), respectively. In both the figures, the high accuracy of those approximate PDFs in predicting their empirical counterparts can be observed. Moreover, Fig. 2(c) shows that, the approximate PDF  $f_a(\tau_j)$  appears to be Gaussian-like in large-scale  $64 \times 64$  and  $128 \times 128$  MIMO systems, as discussed in *Remark*

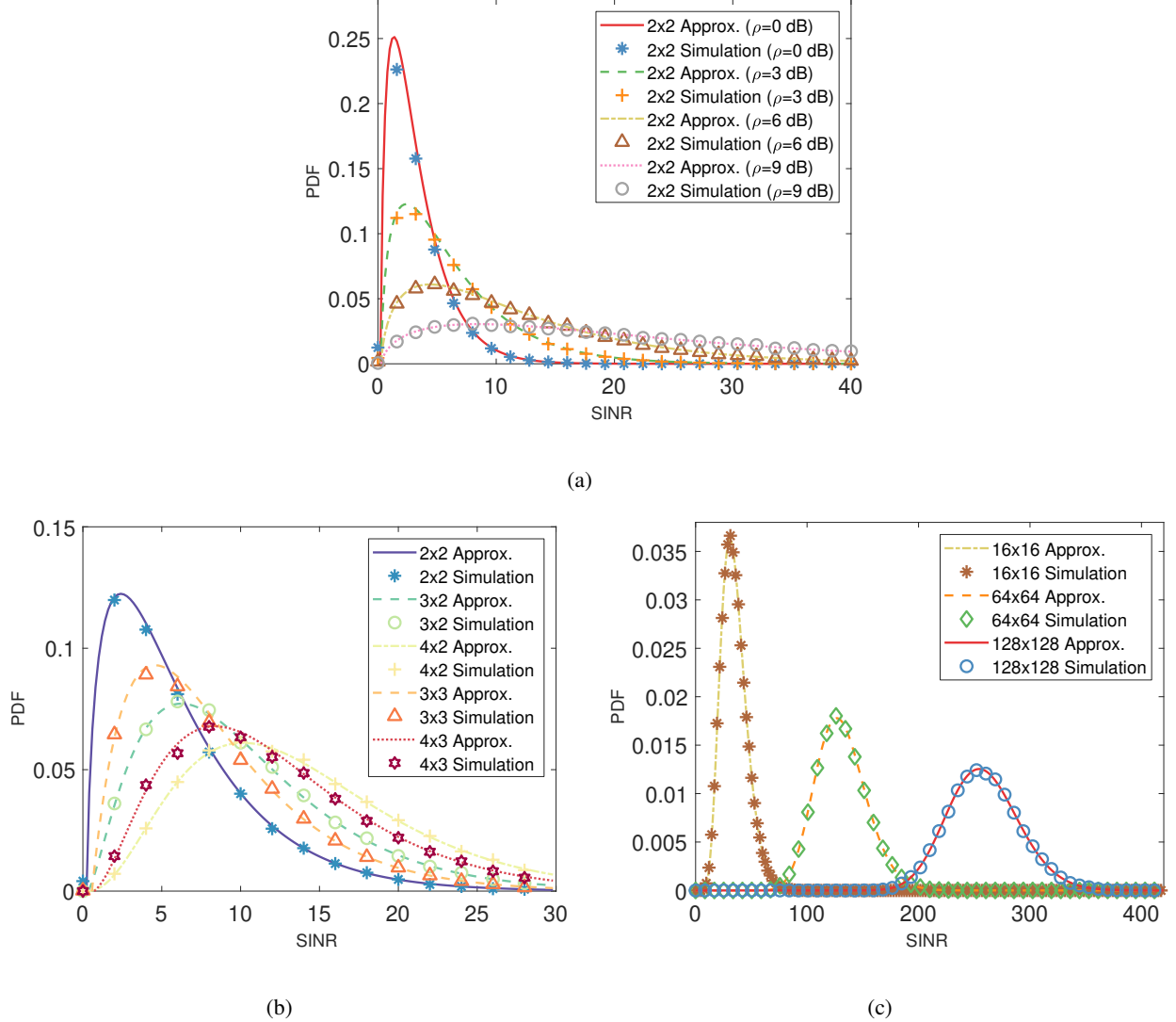


Fig. 2. Approximate PDF  $f_a(\tau_j)$  in (49) and its simulated counterpart as functions of the SINR, against different antenna configurations and SNRs. (a) a  $2 \times 2$  MIMO system with  $\rho = 0$  dB, 3 dB, 6 dB, 9 dB. (b)  $2 \times 2$ ,  $3 \times 2$ ,  $4 \times 2$ ,  $3 \times 3$  and  $4 \times 3$  MIMO systems with  $\rho = 3$  dB. (c)  $16 \times 16$ ,  $64 \times 64$  and  $128 \times 128$  MIMO systems with  $\rho = 3$  dB.

2. To summarize, the condition used to approximate the MGF function  $G(s)$  from (44) to (48), that is, either the SNR  $\rho$  is sufficiently high or the number of receive antennas  $N_r$  is sufficiently larger than  $\frac{N_t-1}{2}$ , is a rather mild one, as the approximate PDF  $f_a(\tau_j)$  is inaccurate only in some special cases, e.g.,  $\rho = 0$  dB and  $N_r = N_t = 2$ .

In the last set of simulations, we investigated the validity of the approximate SER of WLMSE

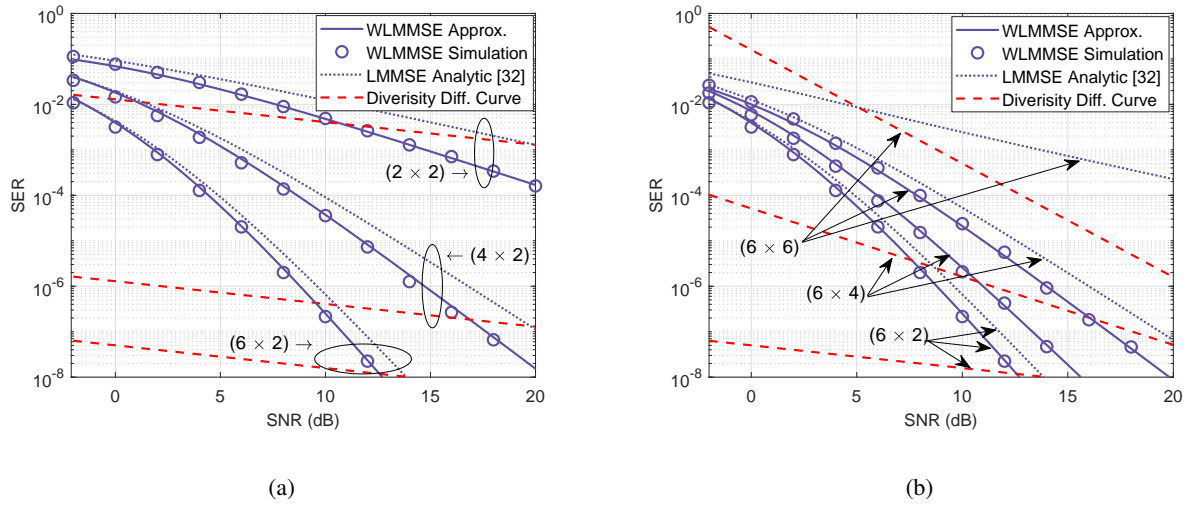


Fig. 3. SERs and diversity gains of WLMMSE and LMMSE MIMO systems as functions of the SNR  $\rho$ . (a)  $2 \times 2$ ,  $4 \times 2$  and  $6 \times 2$  MIMO systems. (b)  $6 \times 2$ ,  $6 \times 4$  and  $6 \times 6$  MIMO systems.

MIMO systems,  $P_e(\rho)$  in (55), and compared it with the analytic SER of LMMSE MIMO systems [32, Eq. (45)], against different levels of noise. The corresponding diversity difference curve between both the WLMMSE and LMMSE receivers was also provided, whose slope represents the diversity gain improvement  $\Delta d$ . This experiment covered five different antenna configurations,  $2 \times 2$ ,  $4 \times 2$ ,  $6 \times 2$ ,  $6 \times 4$  and  $6 \times 6$ , which were classified into two groups, as shown in Fig. 3(a) and Fig. 3(b) separately. The simulation results were obtained by averaging  $8 \times 10^5$  independent realizations, each with  $5 \times 10^3$  transmitted data symbols. The results in Fig. 3 can be interpreted in three aspects. First, for all the five antenna configurations, the approximate SER of the WLMMSE receiver was always closely matched with its empirical counterpart. Second, the WLMMSE receiver provides considerable SER gains over the LMMSE one in different situations. This is expected, because the WL processing framework possesses the modeling advantage over the strictly linear one for the considered MIMO transmission system. Finally, the three diversity difference curves in Fig. 3(a) have an identical slope, indicating the same diversity gain improvement brought by the WLMMSE receiver, while the slope of their

counterparts in Fig. 3(b) gradually increased against the number of transmit antennas  $N_t$ . This phenomenon is in line with the analysis in *Remark 3*.

## VI. CONCLUSION

The post-detection SINR of WLMSE MIMO systems with real-valued constellations has been studied over uncorrelated Rayleigh fading channels. We have first illustrated that the SINR expression can be interpreted in general as a sum of  $N_t$  different and independent gamma random variables, where  $N_t$  is the number of transmit antennas. Furthermore, its analytic PDF for WLMSE MIMO systems with  $N_t = 2, 3$  and an approximate closed form PDF valid for WLMSE MIMO systems of arbitrary size, have been subsequently derived. The so-obtained PDFs have enabled more performance evaluations of WLMSE MIMO receivers in terms of the outage probability, the symbol error rate, and the diversity gain, presented in closed form. Finally, the theoretical findings have been verified through Monte Carlo simulations.

## APPENDIX A

### THE GAMMA RANDOM VARIABLE AND ITS DISTRIBUTION

Let  $\{X_p\} \sim \mathcal{N}(0, \delta^2)$  be a set of i.i.d. Gaussian distributed RVs, where  $p = 1, 2, \dots, P$ , then  $Z = c \sum_{p=1}^P X_p^2$ ,  $\forall c \in \mathbb{R} > 0$ , is a gamma-distributed RV, denoted by  $Z \sim \text{Gamma}(\alpha, \beta)$  with a shape parameter  $\alpha = P/2$  and a scale parameter  $\beta = 2c\delta^2$ , whose PDF is given by

$$f(z) = \frac{1}{\Gamma(\alpha)\beta^\alpha} z^{\alpha-1} e^{-z/\beta}. \quad (62)$$

## APPENDIX B

### THE REAL-VALUED WISHART DISTRIBUTION

A random matrix of form  $\mathbf{Z} = \mathbf{X}\mathbf{X}^\mathcal{T}$ , where  $\mathbf{X} \triangleq [\mathbf{x}_1, \mathbf{x}_2, \dots, \mathbf{x}_Q] \in \mathbb{R}^{P \times Q}$  and the  $P \times 1$  column vectors,  $\mathbf{x}_1, \mathbf{x}_2, \dots, \mathbf{x}_Q$ , are i.i.d. Gaussian random vectors with zero-mean, is called

a real-valued Wishart matrix with  $Q$  degrees of freedom, and is denoted by  $\mathcal{W}_P(\Sigma, Q)$ , in which  $\Sigma \triangleq E[\mathbf{x}_q \mathbf{x}_q^T]$  is the covariance matrix of the column vector  $\mathbf{x}_q$  ( $1 \leq q \leq Q$ ) [50]. Especially, when  $Q \geq P$  and each entry of the matrix  $\mathbf{X}$  is i.i.d.  $\mathcal{N}(0, \delta)$ , the Wishart matrix  $\mathbf{Z} \sim \mathcal{W}_P(\delta \mathbf{I}_P, Q)$  and the PDF of its ordered eigenvalues  $\lambda_1, \lambda_2, \dots, \lambda_P$  ( $\lambda_1 > \lambda_2 > \dots > \lambda_P > 0$ ) is given by [50, Corollary 3.2.19],

$$f_{\Lambda}(\lambda_1, \lambda_2, \dots, \lambda_P) = \frac{\pi^{\frac{P^2}{2}}}{(2\delta)^{\frac{PQ}{2}} \Gamma_P(\frac{P}{2}) \Gamma_P(\frac{Q}{2})} \prod_{p=1}^P e^{-\frac{\lambda_p}{2\delta}} (\lambda_p)^{\frac{Q-P-1}{2}} \prod_{p < u}^P (\lambda_p - \lambda_u). \quad (63)$$

## APPENDIX C

### PROOF OF THE CONVERGENCE OF $f_{N_r \times 2}(\tau_j)$ IN (37)

Let  $A(m)$  denote the infinite series in (33), that is,

$$A(m) = \frac{(N_r - \frac{1}{2})_m \tau_j^m (N_r + m - 1)!}{(N_r)_m 2^m \rho^m m!} U\left(N_r + m, N_r + m + \frac{3}{2}, \frac{\tau_j + 1}{2\rho}\right). \quad (64)$$

Then, we have

$$\begin{aligned} \lim_{m \rightarrow \infty} \frac{A(m+1)}{A(m)} &= \lim_{m \rightarrow \infty} \frac{\frac{(N_r - \frac{1}{2})_{m+1} \tau_j^{m+1} (N_r + m)!}{(N_r)_{m+1} 2^{(m+1)} \rho^{(m+1)} (m+1)!} U\left(N_r + m + 1, N_r + m + \frac{5}{2}, \frac{\tau_j + 1}{2\rho}\right)}{\frac{(N_r - \frac{1}{2})_m \tau_j^m (N_r + m - 1)!}{(N_r)_m 2^m \rho^m m!} U\left(N_r + m, N_r + m + \frac{3}{2}, \frac{\tau_j + 1}{2\rho}\right)} \\ &= \frac{\tau_j}{2\rho} \lim_{m \rightarrow \infty} \frac{U\left(N_r + m + 1, N_r + m + \frac{5}{2}, \frac{\tau_j + 1}{2\rho}\right)}{U\left(N_r + m, N_r + m + \frac{3}{2}, \frac{\tau_j + 1}{2\rho}\right)}. \end{aligned} \quad (65)$$

According to [40, Eq. (13.2.40)], the confluent hypergeometric functions of the second kind in (65) can be equivalently transformed to

$$\begin{aligned} U\left(N_r + m + 1, N_r + m + \frac{5}{2}, \frac{\tau_j + 1}{2\rho}\right) &= \left(\frac{\tau_j + 1}{2\rho}\right)^{-N_r - m - \frac{3}{2}} U\left(-\frac{1}{2}, -N_r - m - \frac{1}{2}, \frac{\tau_j + 1}{2\rho}\right), \\ U\left(N_r + m, N_r + m + \frac{3}{2}, \frac{\tau_j + 1}{2\rho}\right) &= \left(\frac{\tau_j + 1}{2\rho}\right)^{-N_r - m - \frac{1}{2}} U\left(-\frac{1}{2}, -N_r - m + \frac{1}{2}, \frac{\tau_j + 1}{2\rho}\right). \end{aligned} \quad (66)$$

Taking (66) back into the RHS of (65) yields

$$\begin{aligned} \lim_{m \rightarrow \infty} \frac{A(m+1)}{A(m)} &= \left( \frac{\tau_j}{2\rho} \right) \left( \frac{\tau_j+1}{2\rho} \right)^{-1} \lim_{m \rightarrow \infty} \frac{U\left(-\frac{1}{2}, -N_r - m - \frac{1}{2}, \frac{\tau_j+1}{2\rho}\right)}{U\left(-\frac{1}{2}, -N_r - m + \frac{1}{2}, \frac{\tau_j+1}{2\rho}\right)} \\ &= \frac{\tau_j}{\tau_j + 1} \lim_{m \rightarrow \infty} \frac{U\left(-\frac{1}{2}, -N_r - m - \frac{1}{2}, \frac{\tau_j+1}{2\rho}\right)}{U\left(-\frac{1}{2}, -N_r - m + \frac{1}{2}, \frac{\tau_j+1}{2\rho}\right)}. \end{aligned} \quad (67)$$

Based on the recurrent nature of the confluent hypergeometric function of the second kind [40, Eqs. (13.3.9), (13.3.10)], the limitation on the RHS of (67) becomes

$$\begin{aligned} &\lim_{m \rightarrow \infty} \frac{U\left(-\frac{1}{2}, -N_r - m - \frac{1}{2}, \frac{\tau_j+1}{2\rho}\right)}{U\left(-\frac{1}{2}, -N_r - m + \frac{1}{2}, \frac{\tau_j+1}{2\rho}\right)} \\ &= \lim_{m \rightarrow \infty} \frac{(N_r + m + 1)U\left(\frac{1}{2}, -N_r - m - \frac{1}{2}, \frac{\tau_j+1}{2\rho}\right) + \frac{\tau_j+1}{2\rho}U\left(\frac{1}{2}, -N_r - m + \frac{1}{2}, \frac{\tau_j+1}{2\rho}\right)}{(N_r + m + 1)U\left(\frac{1}{2}, -N_r - m - \frac{1}{2}, \frac{\tau_j+1}{2\rho}\right) + \left(\frac{\tau_j+1}{2\rho} - \frac{1}{2}\right)U\left(\frac{1}{2}, -N_r - m + \frac{1}{2}, \frac{\tau_j+1}{2\rho}\right)} \\ &= \lim_{m \rightarrow \infty} \frac{N_r + m + 1 + \frac{\tau_j+1}{2\rho} \frac{U\left(\frac{1}{2}, -N_r - m + \frac{1}{2}, \frac{\tau_j+1}{2\rho}\right)}{U\left(\frac{1}{2}, -N_r - m - \frac{1}{2}, \frac{\tau_j+1}{2\rho}\right)}}{N_r + m + 1 + \left(\frac{\tau_j+1}{2\rho} - \frac{1}{2}\right) \frac{U\left(\frac{1}{2}, -N_r - m + \frac{1}{2}, \frac{\tau_j+1}{2\rho}\right)}{U\left(\frac{1}{2}, -N_r - m - \frac{1}{2}, \frac{\tau_j+1}{2\rho}\right)}}. \end{aligned} \quad (68)$$

According to [40, Eqs. (13.5.3), (13.5.4)],  $\forall N_r, m \in \mathbb{Z}^+$ , the term  $\frac{U\left(\frac{1}{2}, -N_r - m + \frac{1}{2}, \frac{\tau_j+1}{2\rho}\right)}{U\left(\frac{1}{2}, -N_r - m - \frac{1}{2}, \frac{\tau_j+1}{2\rho}\right)}$  is a continued fraction that converges to a meromorphic function of  $\phi$ , denoted by  $B(\phi)$ , where  $\phi \triangleq \frac{\tau_j+1}{2\rho}$ , then (68) becomes

$$\lim_{m \rightarrow \infty} \frac{U\left(-\frac{1}{2}, -N_r - m - \frac{1}{2}, \frac{\tau_j+1}{2\rho}\right)}{U\left(-\frac{1}{2}, -N_r - m + \frac{1}{2}, \frac{\tau_j+1}{2\rho}\right)} = \lim_{m \rightarrow \infty} \frac{N_r + m + 1 + \phi B(\phi)}{N_r + m + 1 + (\phi - \frac{1}{2})B(\phi)} = 1. \quad (69)$$

Finally, taking (69) into (67), we arrive at

$$\lim_{m \rightarrow \infty} \frac{A(m+1)}{A(m)} = \frac{\tau_j}{\tau_j + 1} < 1, \quad (70)$$

which completes the proof of the convergence of (37). ■

## REFERENCES

- [1] Z. Li, W. Deng, W. Pei, Y. Xia, C. Zhu, and D. P. Mandic, “SINR analysis of MIMO systems with widely linear MMSE receivers for the reception of real-valued constellations,” in *Proc. IEEE Int. Symp. Pers. Indoor Mob. Radio Commun. (PIMRC)*, London, United Kingdom, 2020, pp. 1–5.
- [2] Z. Guo and P. Nilsson, “Algorithm and implementation of the K-best sphere decoding for MIMO detection,” *IEEE J. Select. Areas Commun.*, vol. 24, no. 3, pp. 491–503, Mar. 2006.
- [3] A. Mobasher, M. Taherzadeh, R. Sotirov, and A. K. Khandani, “A near-maximum-likelihood decoding algorithm for MIMO systems based on semi-definite programming,” *IEEE Trans. Inf. Theory*, vol. 53, no. 11, pp. 3869–3886, Nov. 2007.
- [4] M. Jankiraman, *Space-time Codes and MIMO Systems*. Artech House, 2004.
- [5] H. Sampath, P. Stoica, and A. Paulraj, “Generalized linear precoder and decoder design for MIMO channels using the weighted MMSE criterion,” *IEEE Trans. Commun.*, vol. 49, no. 12, pp. 2198–2206, Dec. 2001.
- [6] E. A. Jorswieck and H. Boche, “Transmission strategies for the MIMO MAC with MMSE receiver: Average MSE optimization and achievable individual MSE region,” *IEEE Trans. Signal Process.*, vol. 51, no. 11, pp. 2872–2881, Nov. 2003.
- [7] G. D. Golden, C. J. Foschini, R. A. Valenzuela, and P. W. Wolniansky, “Detection algorithm and initial laboratory results using V-BLAST space-time communication architecture,” *Electron. Lett.*, vol. 35, no. 1, pp. 14–16, Jan. 1999.
- [8] R. Ran, J. Wang, S. K. Oh, and S. N. Hong, “Sparse-aware minimum mean square error detector for MIMO systems,” *IEEE Commun. Lett.*, vol. 21, no. 10, pp. 2214–2217, Oct. 2017.
- [9] J. W. Choi and B. Shim, “Detection of large-scale wireless systems via sparse error recovery,” *IEEE Trans. Signal Process.*, vol. 65, no. 22, pp. 6038–6052, Nov. 2017.
- [10] P. Schreier and L. Scharf, “Second-order analysis of improper complex random vectors and processes,” *IEEE Trans. Signal Process.*, vol. 51, no. 3, pp. 714–725, Mar. 2003.
- [11] D. P. Mandic and S. L. Goh, *Complex Valued Nonlinear Adaptive Filters: Noncircularity, Widely Linear and Neural Models*. John Wiley & Sons, 2009.
- [12] B. Picinbono and P. Chevalier, “Widely linear estimation with complex data,” *IEEE Trans. Signal Process.*, vol. 43, no. 8, pp. 2030–2033, Aug. 1995.
- [13] Y. Xia and D. Mandic, “Augmented performance bounds on strictly linear and widely linear estimators with complex data,” *IEEE Trans. Signal Process.*, vol. 66, no. 2, pp. 507–514, Jan. 2018.
- [14] H. Gerstacker, R. Schober, and A. Lampe, “Receivers with widely linear processing for frequency-selective channels,” *IEEE Trans. Commun.*, vol. 51, no. 9, pp. 1512–1523, Sep. 2003.
- [15] R. Schober, W. H. Gerstacker, and L. H. Lampe, “Data-aided and blind stochastic gradient algorithms for widely linear MMSE MAI suppression for DS-CDMA,” *IEEE Trans. Signal Process.*, vol. 52, pp. 746–756, Mar. 2004.

- [16] D. Mattera, L. Paura, and F. Sterle, "Widely linear MMSE equaliser for MIMO linear time-dispersive channel," *Electron. Lett.*, vol. 39, no. 20, pp. 13–14, Oct. 2003.
- [17] F. Sterle, "Widely linear MMSE transceivers for MIMO channels," *IEEE Trans. Signal Process.*, vol. 55, no. 8, pp. 4258–4270, Aug. 2007.
- [18] K. Kuchi and V. K. Prabhu, "Performance evaluation for widely linear demodulation of PAM/QAM signals in the presence of Rayleigh fading and co-channel interference," *IEEE Trans. Commun.*, vol. 57, no. 1, pp. 183–193, Jan. 2009.
- [19] P. Chevalier, R. Chauvat, and J.-P. Delmas, "Enhanced widely linear filtering to make quasi-rectilinear signals almost equivalent to rectilinear ones for SAIC/MAIC," *IEEE Trans. Signal Process.*, vol. 66, no. 6, pp. 1438–1453, Mar. 2018.
- [20] P. Chevalier and F. Dupuy, "Widely linear Alamouti receiver for the reception of real-valued constellations corrupted by interferences—The Alamouti-SAIC/MAIC concept," *IEEE Trans. Signal Process.*, vol. 59, no. 7, pp. 3339–3354, Jul. 2011.
- [21] S. Zarei, W. Gerstacker, and R. Schober, "Low-complexity widely-linear precoding for downlink large-scale MU-MISO systems," *IEEE Commun. Lett.*, vol. 19, no. 4, pp. 665–668, Apr. 2015.
- [22] W. Deng, Z. Li, Y. Xia, K. Wang, and W. Pei, "A widely linear MMSE anti-collision method for multi-antenna RFID readers," *IEEE Commun. Lett.*, vol. 23, no. 4, pp. 644–647, Apr. 2019.
- [23] A. S. Aghaei, K. N. Plataniotis, and S. Pasupathy, "Widely linear MMSE receivers for linear dispersion space-time block-codes," *IEEE Trans. Wireless Commun.*, vol. 9, no. 1, pp. 8–13, Jan. 2010.
- [24] Y. Ding, N. Li, Y. Wang, S. Feng, and H. Chen, "Widely linear sphere decoder in MIMO systems by exploiting the conjugate symmetry of linearly modulated signals," *IEEE Trans. Signal Process.*, vol. 64, no. 24, pp. 6428–6442, Dec. 2016.
- [25] P. Schreier and L. Scharf, *Statistical Signal Processing of Complex-Valued Data: The Theory of Improper and Noncircular Signals*. Cambridge University Press, 2010.
- [26] P. Chevalier, J.-P. Delmas, and A. Oukaci, "Properties, performance and practical interest of the widely linear MMSE beamformer for nonrectilinear signals," *Signal Process.*, vol. 97, pp. 269–281, Apr. 2014.
- [27] H. V. Poor and S. Verdú, "Probability of error in MMSE multiuser detection," *IEEE Trans. Inf. Theory*, vol. 43, no. 3, pp. 858–871, May 1997.
- [28] D. N. Tse and S. V. Hanly, "Linear multiuser receivers: Effective interference, effective bandwidth and user capacity," *IEEE Trans. Inf. Theory*, vol. 45, no. 2, pp. 641–657, Mar. 1999.
- [29] P. Li, D. Paul, R. Narasimhan, and J. Cioffi, "On the distribution of SINR for the MMSE MIMO receiver and performance analysis," *IEEE Trans. Inf. Theory*, vol. 52, no. 1, pp. 271–286, Jan. 2006.
- [30] N. Kim, Y. Lee, and H. Park, "Performance analysis of MIMO system with linear MMSE receiver," *IEEE Trans. Wireless Commun.*, vol. 7, no. 11, pp. 4474–4478, Nov. 2008.
- [31] W. Kim, N. Kim, H. Chung, and H. Lee, "SINR distribution for MIMO MMSE receivers in transmit-correlated Rayleigh channels: SER performance and high-SNR power allocation," *IEEE Trans. Veh. Technol.*, vol. 62, no. 9, pp. 4083–4087, Oct. 2013.

- [32] H. Lim and D. Yoon, "On the distribution of SINR for MMSE MIMO systems," *IEEE Trans. Commun.*, vol. 67, no. 6, pp. 4035–4046, Jun. 2019.
- [33] J. Yang and R. C. de Lamare, "Widely-linear minimum-mean-squared error multiple-candidate successive interference cancellation for multiple access interference and jamming suppression in direct-sequence code-division multiple-access systems," *IET Signal Process.*, vol. 9, no. 1, pp. 73–81, Feb. 2015.
- [34] R. Couillet and M. Debbah, *Random Matrix Methods for Wireless Communications*. Cambridge University Press, 2011.
- [35] G. H. Golub and C. F. V. Loan, *Matrix Computations*. Johns Hopkins Univ. Press, 1996.
- [36] G. P. Efthymoglou, T. Piboongunon, and V. A. Aalo, "Performance of DS-CDMA receivers with MRC in nakagami-m fading channels with arbitrary fading parameters," *IEEE Trans. Veh. Technol.*, vol. 55, no. 1, pp. 104–114, Jan. 2006.
- [37] R. A. Horn and C. Johnson, *Matrix Analysis*. Cambridge university press, 2012.
- [38] V. A. Aalo, T. Piboongunon, and G. P. Efthymoglou, "Another look at the performance of MRC schemes in Nakagami-m fading channels with arbitrary parameters," *IEEE Trans. Commun.*, vol. 53, no. 12, pp. 2002–2005, Dec. 2005.
- [39] I. S. Ansari, F. Yilmaz, and M.-S. Alouini, "New results on the sum of Gamma random variates with application to the performance of wireless communication systems over Nakagami-m fading channels," *Trans. Emerg. Telecommun. Technol.*, vol. 28, no. 1, pp. 1–14, Nov. 2014.
- [40] F. W. Olver, D. W. Lozier, R. F. Boisvert, and C. W. Clark, *NIST Handbook of Mathematical Functions Hardback and CD-ROM*. Cambridge Univ. Press, 2010.
- [41] A. P. Prudnikov, I. U. A. Brychkov, and O. I. Marichev, *Integrals and Series, Volume 3: More Special Functions*. Gordon and Breach Science, 1990.
- [42] P. G. Moschopoulos, "The distribution of the sum of independent gamma random variables," *Ann. Inst. Statist. Math.*, vol. 37, no. 1, pp. 541–544, Dec. 1985.
- [43] A. Edelman, "The distribution and moments of the smallest eigenvalue of a random matrix of Wishart type," *Lin. Alg. Appl.*, vol. 159, pp. 55–80, Dec. 1991.
- [44] D. von Rosen, "Moments for the inverted Wishart distribution," *Scand. J. Stat.*, vol. 15, no. 2, pp. 97–109, Jan. 1988.
- [45] L. M. Leemis and J. T. McQueston, "Univariate distribution relationships," *The Am. Stat.*, vol. 62, no. 1, pp. 45–53, 2008.
- [46] M. K. Simon and M.-S. Alouini, *Digital Communication over Fading Channels*. John Wiley & Sons, 2005.
- [47] J. Proakis, *Digital Communications*. McGraw-Hill, 2001.
- [48] M. Chiani, D. Dardari, and M. K. Simon, "New exponential bounds and approximations for the computation of error probability in fading channels," *IEEE Trans. Wireless Commun.*, vol. 2, no. 4, pp. 840–845, Jul. 2003.
- [49] L. Zheng and D. N. Tse, "Diversity and multiplexing: A fundamental tradeoff in multiple-antenna channels," *IEEE Trans. Inf. Theory*, vol. 49, no. 5, pp. 1073–1096, May 2003.
- [50] R. J. Muirhead, *Aspects of Multivariate Statistical Theory*. John Wiley & Sons, 2009.